

Low-Frequency Vibrational Motion of Arctic Pack Ice

J. P. DUGAN,¹ R. L. DiMARCO, AND W. W. MARTIN

Areté Associates, Arlington, Virginia

The mechanisms responsible for vibrational motions of Arctic ice at frequencies below about 100 Hz are known to be a combination of wave types, namely, gravity waves, flexural waves, and a variety of acoustic and/or elastic waves. Surface motion measurements using geophones and accelerometers on multiyear pack ice are used to establish the energy level of these motions and to differentiate between the different modes of propagation. Gravity waves are dominant below about 0.05 Hz, with their direction and dispersion relation being confirmed with vector measurements of acceleration from two stations. Motions driven by surface pressure fluctuations in the local wind appear at somewhat higher frequencies up to about 0.3 Hz and are particularly evident on thinner first-year ice during periods of high wind. The band from 0.1 to 10 Hz comprises mainly flexural waves, as determined by their dispersion relation, and these are prominent during local ridge building events. At frequencies above 10 Hz, there is a combination of acoustic and flexural modes of propagation, with one or the other being dominant during specific environmental events. The probability density function of power in octave wide bands is approximately lognormal as a result of the high level of intermittence of local events. The variance in power level is significantly smaller for waterborne noise from more distant sources. Specific examples are used to illustrate the nature of the events.

INTRODUCTION

Measurements of the vibrational motion of Arctic ice have been available for many years. Low-frequency oscillations due to gravity and elastic restoring forces were known to be possible modes of wave propagation from explosive sources on ice in lakes [Ewing and Crary, 1934] and on Arctic pack ice [Oliver *et al.*, 1954]. Crary *et al.* [1952] evidently first observed gravity waves as naturally occurring oscillations in the pack ice far from the open ocean. Crary *et al.* [1952] and Crary [1956] used gravimeter measurements to show that these wave motions occurred near a frequency of 0.03 Hz, and Hunkins [1962] showed that these waves were propagating at a speed at least consistent with surface waves. The waves were presumed to be generated elsewhere, from the open ocean or perhaps from other ice-covered regions having high winds, and to be propagating through the region of the measurements. The energy level of the motions, however, also showed a dependence upon the local wind field, and Hunkins [1962] suggested that the waves could be generated more locally by the wind when it exceeded a critical value equal to the minimum phase speed of flexural-gravity waves. Hunkins reported an increase in the energy level in the presence of high wind but did not specifically identify changes in the frequency content of the waves, a change which is expected from the physics of the situation [DiMarco *et al.*, 1991]. He also made a first attempt to construct a power spectrum of surface velocity across several decades of frequency. LeSchack and Haubrich [1964] confirmed the general form of the frequency spectrum in pack ice and on an ice shelf, both of which exhibit a prominent peak in level near 0.025 Hz due to the gravity waves. They also found an increase in energy at frequencies lower than the gravity wave peak in the presence of high wind, a result which was not explained.

Robin [1963] reported gravity wave spectra measured from a ship at various distances into pack ice from the ice edge. These spectra exhibited a sharp decay in the high frequencies with increasing distance from the open sea, and significance was attached to the shortest waves requiring flexure of the ice. The physics of swell attenuation, especially in the marginal ice zone, has been studied extensively by Wadhams and co-workers (see Wadhams [1973] or Wadhams *et al.* [1988], for example). They have confirmed the strong attenuation of the shortest waves by measuring attenuation coefficients at various locations and times, and have exercised various models of the decay mechanism. It seems certain that swell from the open ocean propagates into the ice pack, losing its higher-frequency components as a result of one or more of the hypothesized dissipative mechanisms. The low-frequency waves measured by Hunkins [1962] perhaps were the remainder of waves coming from the marginal ice zone, although the association with this source was not certain since the direction of propagation was not clearly determined and his station Alpha was about as far as possible from the open ocean.

Generation of ice motions by the local wind has been hypothesized by Hunkins [1962], as noted above, and models and measurements of this mechanism have been reported more recently by Squire [1986] and Crocker and Wadhams [1988]. These analyses basically confirm the importance of a threshold wind speed for the generation of significant wave motions in the ice, but direct predictions and corroborative measurements of spectral levels and shapes have not been made. DiMarco *et al.* [1991] have shown that large motions can be generated on ice on a frozen lake when the wind speed is still below the critical speed (i.e., the minimum phase speed of flexural-gravity waves). The mechanism causing the motions is the passage of pressure fluctuations in the atmospheric turbulent boundary layer across the surface of the ice. This mechanism should be operable in the Arctic. In this model, the pressure field is assumed to satisfy Taylor's hypothesis, that is, to be frozen in the flow moving with the mean wind speed over the ice. The most important predictions of the model are the very strong dependence of

¹Now at European Office, Office of Naval Research, London.

Copyright 1992 by the American Geophysical Union.

ice motion variance upon the mean wind speed and the existence of a strong spectral peak near a critical frequency. This critical frequency is the frequency of the waves having the slowest phase speed on the flexural-gravity wave dispersion surface and is of the order of 0.1 Hz for typical Arctic pack ice. Thus ice motions in the frequency band near 0.1 Hz can be expected to occur during high winds.

At higher frequencies, there have been a number of studies of flexural and acoustic modes of propagation that the ice plate can support, including those of *Ewing and Crary* [1934], *Oliver et al.* [1954], and *Hunkins* [1960]. These studies typically have involved wave propagation associated with explosive sources. A number of analyses of ambient sound in the water below pack ice have found that several distinct sources of noise are present. A near-surface cracking mechanism is present when the surface cools significantly, and this causes a reasonably broad peak in the spectrum in the vicinity of 200–400 Hz [cf. *Milne et al.*, 1967; *Milne*, 1972]. In addition, the wind can cause noise in a broad frequency band above several kilohertz by blowing ice crystals across the surface [cf. *Ganton and Milne*, 1965; *Milne et al.*, 1967]. Finally, pack ice is subject to episodes of geometric distortion involving large-scale shear or compression, and these events are the source of much of the noise, particularly at frequencies in the 0.1- to 100-Hz band. *Crary* [1955] has localized discrete fracture events by observing the travel time difference of the elastic and flexural waves, and *Smirnov and Lin'kov* [1967] have localized glacier calving events by similar analyses.

Buck and Wilson [1986] have studied the noise caused by ridge building, with the conclusion that most of the noise is generated by subsurface sources. In addition, they discussed a potential difference between noise due to nearby events and that due to remote events. This differentiation was based upon the point statistics of the measured sound level, with levels above the ninety-fifth percentile being assumed to be nearby and those nearer the mean level being from elsewhere. *Dyer* [1983] and *Makris and Dyer* [1986] have published a spectrum of sound level from a suspended hydrophone across the whole frequency band from 0.01 Hz to 10 kHz. The spectrum shows a significant peak near 10 Hz which is concluded to be a result of the omnipresent noise due to ice ridging. The spectral level rolls off monotonically at frequencies higher than 20 Hz, except in the presence of higher-frequency sources as mentioned above. The spectrum also begins to roll off at frequencies less than 10 Hz, but hydrophones suspended from the ice are subject to contamination by several extraneous effects. High-amplitude spectral peaks often appear in the data in the vicinity of 1 Hz, caused by resonant strumming of the suspension cable due to the passing water flow. The spectra can also exhibit a strong increase in level at even lower frequencies, which *Dyer* [1983] has suggested is due to the dynamic pressure of the turbulence in the water as it passes the transducer. Using the variance in the 10- to 20-Hz band as a measure of the energy in the 1- to 100-Hz band, *Makris and Dyer* [1986] obtain a significant correlation with dynamical stresses in the ice caused by large-scale environmental loading of wind and relative current. *Pritchard* [1984] has modeled this effect, with source intensity being linearly dependent upon the rate of dissipation of energy in large scale ice deformations, and found a significant correlation in the Arctic Ice Dynamics Joint Experiment (AIDJEX) data set.

There have been much more limited measurements of actual ice motion in the band of frequencies between 0.1 and 10 Hz, which spans the acoustic/elastic and flexural wave regimes, for known ice ridging events. *Greene and Buck* [1964] have measured both ice motions and acoustic intensity at somewhat higher frequencies. They measured the vertical component of ice velocity with a seismometer in the band from 25 Hz to 1 kHz, and have found an average spectrum over 15 days to be monotonically decreasing with frequency. The peak was at the lowest frequency resolved (25 Hz), and the roll-off was about 3 dB/octave, which was significantly less than that of a nearby hydrophone suspended below the ice. Variations about the mean power level were about equally distributed over frequency, and little association of the level was found with wind speed, except for marginal correlation for a 24-hour delay.

This paper is the result of an attempt to identify the sources of vibrational motions in pack ice across the frequency band 0.01–100 Hz. We document spectral results from geophones and accelerometers on the ice, with the modest goal of determining the various environmental sources of ice motions and determining the frequency band in which each is dominant.

INSTRUMENTATION AND DATA

Two instrument stations were maintained on pack ice for over 2 weeks in the spring season near 84°N, north of Greenland. Each station contained a three-axis geophone and a three-axis accelerometer. The geophones were rugged Litton Resources model 1033, which have a natural frequency of 8 Hz, a flat frequency response to several kilohertz, and a monotonic roll off below 8 Hz of 12 dB/octave. A preamplifier with 50 dB of gain was provided at the instrument, and the signal was hardwired into a warm tent where postamplification was applied as required and anti-alias filtering, digitization, and recording were effected. With care taken in the gain, the signal was maintained above system noise most of the time at frequencies above about 0.1 Hz. The accelerometers were Sundstrand Model QA1400 which also were preamplified near the sensors and digitized and recorded in the tent. The data from the vertical channels were integrated to provide measurements of vertical velocity, and the horizontal channels were rescaled to provide estimates of ice tilt. The ice tilt angle θ was calculated from $\theta = \arctan(a/g)$, where a is the measured horizontal acceleration and g is the gravity constant. Both the geophones and accelerometers were frozen into the surface of the ice and covered with snow to protect them from direct action of the wind. Finally, the local atmospheric conditions including air temperature, wind speed, and barometric pressure were recorded continuously, and thorough surveys of the ice constituting the floe were made.

The data from the motion sensors were low-pass filtered at 1, 10, or 100 Hz and sampled at twice these frequencies, with the choice of operating band being made by the operator. Eighteen days of almost continuous recording were completed at the 1-Hz rate. In addition, 112 hours of geophone data were obtained at the 10-Hz rate and 2.5 hours at the 100-Hz rate, spread nonuniformly throughout the period.

The bulk of the measurements were made on a multiyear floe about 2 km across. One sensor station was installed near the center of the floe most of the time, where the mean

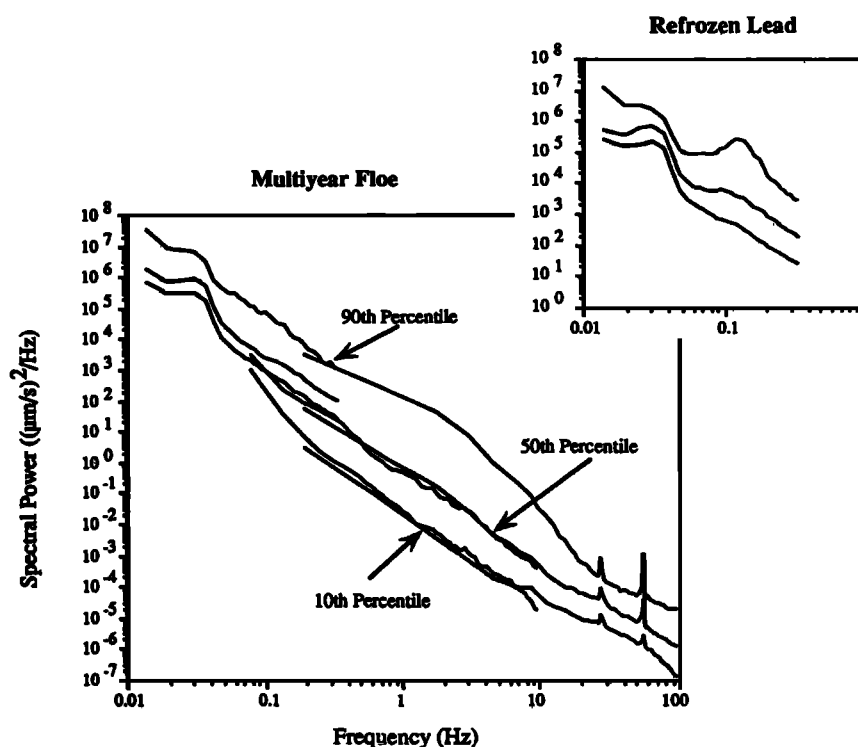


Fig. 1. Lines represent the tenth, fiftieth, and ninetieth percentiles of all vertical velocity spectra on the multiyear pack ice. Spectral estimates were calculated at each frequency and ordered in magnitude to obtain the plotted levels. No frequency averaging has been applied. Data below 0.3 Hz are from an accelerometer, while higher-frequency data are from a geophone. There are a total of 420 spectral estimates below 1 Hz, 1122 estimates in the band from 0.1 to 10 Hz, and 246 estimates for frequencies higher than 10 Hz. The inset is from a vertical accelerometer on first-year ice (see text).

thickness was 3.6 m with an rms of 0.5 m, as determined by cores and drill holes. The nominal value of Young's modulus from the cores was 2.2 GPa, and the value of the flexural rigidity was 9.6 GN m. The preamplifiers were provided so that the sensors could be moved at will on long cables. Measurements at 1 Hz were also made on a refrozen lead which was 1 m thick. More limited measurements were made at other locations on the experiment floe and on adjacent floes. During the data collection period, the floe experienced episodes of high shear along one side, with intermittent shear ridging events. There were several wind events with speeds to 12 m/s, and the air temperature trended warmer in the 18 days of measurements from -33° to -10°C .

RESULTS

The measured level of motion varied considerably during the period of observations. Figure 1 is a spectrum of vertical velocity across the whole frequency band resolved by the measurements. It is not the typical frequency spectrum but has been constructed from samples of the spectrum at the three sample rates and the segment durations shown in Table 1. Seven spectral estimates of 1024-point subsections were computed and ensemble averaged for each data segment. At each frequency, the tenth, fiftieth, and ninetieth percentile spectral levels were computed from the set of ensemble averages, and these levels were plotted as the continuous lines in the figure. It should be noted that since the percentiles were computed separately at each frequency, no individual ensemble spectrum is likely to look exactly like any of

the curves in the figure. These curves, for example, are much smoother than any one of the ensemble spectra, but the general spectral forms are retained. Also, since the motions were not stationary and time intervals of the data collection periods in different frequency bands were not the same, as shown in Table 1, the percentiles in the different bands are not identical where they overlap. There is a good overlap of the 10- and 100-Hz levels, but there is some disagreement in the overlap near 0.1 Hz. This latter misalignment is especially apparent in the tenth percentile curve between 0.1 and 1 Hz. The higher level obtained from the vertical accelerometer in this band is due to instrument noise.

The data exhibit a peak near 0.03 Hz which is consistent with the gravity wave peak observed by previous investigators [e.g., *Crary et al.*, 1952]. There also is a peak in the vicinity of 0.1 Hz (shown in the inset in Figure 1) on refrozen lead ice. The spectral level at this frequency is highly variable, and the peak will be seen to be due to the local wind. The broad, highly variable region in the decade of

TABLE 1. Summary of Observations

Frequency Band, Hz	Data Length, s	Number of Segments
0.01–0.4	3600	420
0.08–10	360	1122
0.2–100	36	246

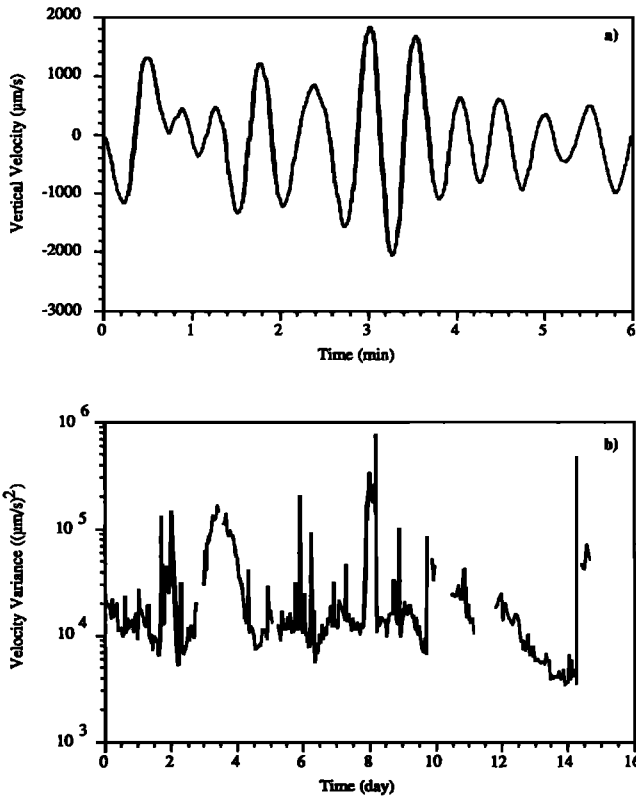


Fig. 2. Vertical velocity data from an accelerometer on multi-year ice. (a) Sample time series. (b) Time series of variance in the band 0.02–0.06 Hz for the whole data collection period.

bandwidth near 1 Hz is flexural waves, and the less energetic band above 10 Hz is mostly elastic waves. The narrow lines near 30 and 60 Hz are due to electronic noise caused by the camp electrical generator. In the following sections, each of these mechanisms will be discussed in turn.

Gravity Waves

A time series of vertical velocity data of a few minutes' duration is shown in Figure 2a. The velocity is dominated by the quasi-periodic motions which produce the spectral peak in the vicinity of 0.02–0.06 Hz. The direction of these waves has been determined from the ratio of the energy in the two horizontal accelerometer channels, i.e., the tilt. The predominant direction indicated that these waves were coming from the closest point of the marginal ice zone, Fram Strait, as shown in Figure 3. Using the observed direction, the

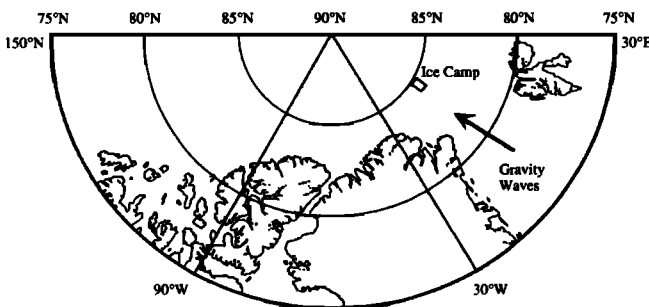


Fig. 3. Locator map for the instrumented camp. The arrow indicates the direction of propagation of the waves near 0.03 Hz.

wavelength (and hence the wave speed) was calculated from the phase function of the cross-spectrum between the vertical sensors on two spatially separated stations. The phase speed is plotted versus frequency in Figure 4 as asterisks on the left side. The smooth solid lines represent the theoretical dispersion relation for flexural-gravity waves; the branch on the left has gravity as the restoring force, while the branches on the right side have elastic flexure as the restoring force. The waves shown in Figure 2a are apparently gravity waves, since the plotted points are in excellent agreement with the predicted dispersion curve. (On both sides of this wave band of 0.02–0.05 Hz, other noise sources lower the coherence between the two sensors markedly, and the data for the indicated phase speed become very noisy.) The dispersion relation is much more accurately confirmed with the present data than by *Hunkins* [1962]. The conclusion that these are gravity waves is also supported by the observed pattern of particle orbits. The cross spectrum between the vertical and horizontal channels demonstrates that the vertical acceleration leads the tilt by 90°, and the spectra in Figure 5 show that the vertical and horizontal velocities are the same, as anticipated for gravity waves.

The observations of the wave propagation characteristics are in good agreement with the theory for gravity waves and, combined with their direction of travel, indicate that the motions are the remainder of surface swell propagating into the ice pack from the open ocean. The time series of variance in the gravity wave band over the period of the experiment (Figure 2b) shows that the variability in the energy is dominated by a few large events of limited duration. The local increase in days 3–4 is consistent with gravity waves produced by storms in the North Atlantic well south of Fram Strait, but the shorter-period events are of undetermined origin. From the fiftieth percentile curve in Figure 1, we may estimate the median vertical displacements of the ice

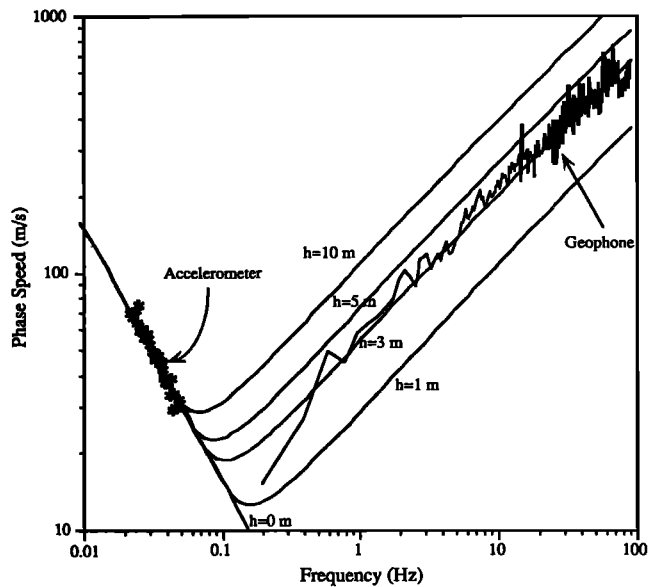


Fig. 4. Dispersion relation for flexural-gravity waves. Smooth line is theory for ice of several thicknesses (and Young's modulus of 2.2 GPa), and data are from phase function of the cross spectrum from pairs of sensor stations. Data toward left side are from accelerometers spaced 300 m apart and those toward right side are from geophones spaced 30 m apart.

surface. The peak value in the spectrum near 0.03 Hz is equivalent to an rms displacement of 1.2 cm. This amplitude is larger than those found by *Hunkins* [1962], although our measurement site was closer to the marginal ice zone and should thus be closer to the open ocean value. *Munk et al.* [1959] present displacement spectra obtained by sea level measurements from several locations in ice-free waters. Their observed rms displacements range from 0.17 cm to 5.4 cm, and our observations fall comfortably within this range.

There are two additional comments worthy of note concerning the motions in this frequency band. The amplitudes measured at separate sensor stations at the same time are identical within the accuracy of the measurements, independent of whether the sensors were on different floes or whether they were on thick or thin ice. Also, the spectra cut off sharply at the high-frequency side of the peak, close to the point in the dispersion curve where ice flexure occurs, as expected from the dissipative mechanisms associated with ice flexure as discussed by *Wadhams* [1973], among others. Both of these results are expected for gravity waves. The observed spectral levels at lower frequency than the wave peak are thought to be due to low-frequency drift in the sensors and electronics, and not real ice motions.

Wind-Driven Motions

Moving to frequencies above the sharp roll-off in energy at the high-frequency side of the gravity wave peak, we sometimes observe an additional peak due to wind-induced motions. These are present only during high-wind periods on thinner ice. The spectrum in the inset in Figure 1 is from a sensor on a 1-m-thick refrozen lead. This exhibits a peak near 0.1 Hz, and the level varies markedly, as is shown by the difference between the fiftieth and ninetieth percentile curves. Figure 6 shows a sample spectrum of the vertical velocity of this sensor. The peak near 0.03 Hz represents the long gravity waves discussed previously, and the level on thin ice is identical to that of simultaneous measurements on the thicker ice floe as noted previously. The peak near 0.1 Hz is a result of wind-driven motions, and the behavior on thin ice is quite different from that on thick ice. The smooth line is the prediction from the model of *DiMarco et al.* [1991] for the average wind speed observed at this time. The model predicts the location of the peak and the shape; the

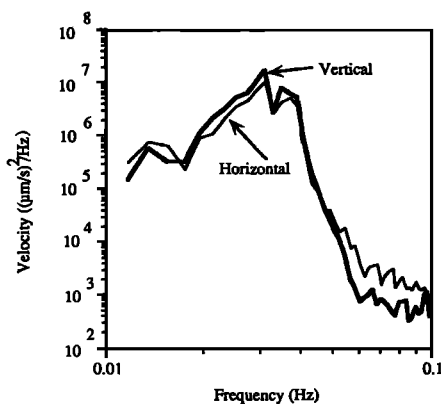


Fig. 5. Spectra for horizontal and vertical velocity calculated from accelerometers on multiyear ice. Equal amplitude in the band near 0.03 Hz supports propagation mode as gravity waves.

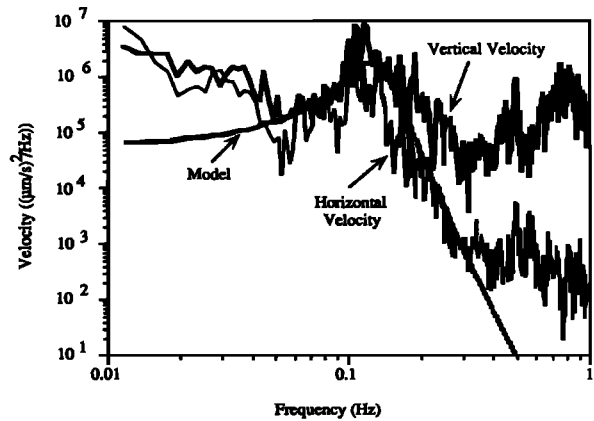


Fig. 6. Spectra of horizontal and vertical velocity calculated from accelerometers on 1-m-thick first-year ice. The peak near 0.03 Hz is due to gravity waves, and that near 0.2 Hz is due to wind. Data below 0.02 Hz are contaminated by sensor noise. The smooth line from theory of *DiMarco et al.* [1991] for wind speed of 12 m/s (see text).

overall amplitude is arbitrary. The agreement with the model leads us to conclude that these motions are driven by pressure fluctuations in the atmospheric boundary layer.

One-hour averages of the variance in the band 0.06–0.3 Hz have been calculated and are plotted along with the 1-hour average wind speed in Figure 7. For low wind there is considerable scatter in the result due to the presence of other mechanisms dominating the tilt variance, especially short periods of waves due to ridging events (to be discussed

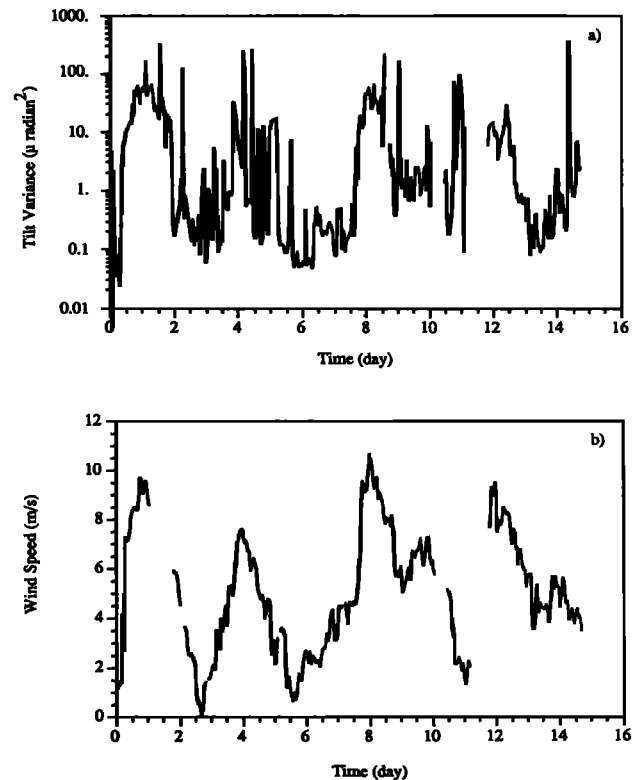


Fig. 7. (a) Time series of variance of ice tilt (from horizontal accelerometers on a 1-m-thick refrozen lead) in the 0.06- to 0.3-Hz band, and (b) mean wind speed. Variance and mean computed in 1-hour sections of data.

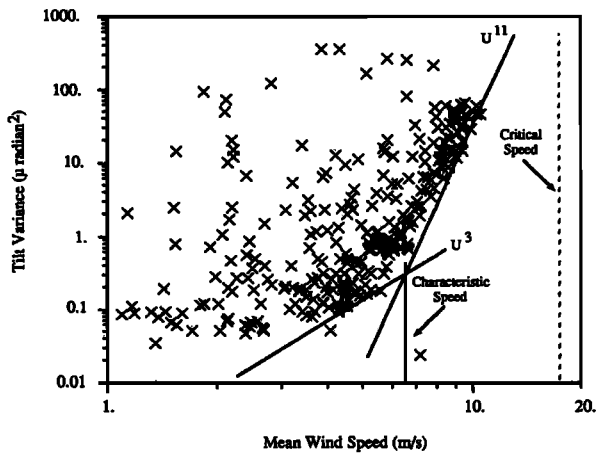


Fig. 8. Scatter plot of mean wind speed versus tilt variance in the 0.06- to 0.3-Hz band; same data as in Figure 7. Power laws and critical and characteristic speeds determined following *DiMarco et al.* [1991].

later). However, at higher wind speeds, the correlation is obvious. A scatter plot of 1-hour samples of tilt variance versus wind speed is shown in Figure 8, and the smooth lines again are predictions from the *DiMarco et al.* [1991] model. In comparing observations with the theory, we have taken some latitude in locating the characteristic speed where the break in the slope of the line occurs. There clearly is a grouping of data above the lines, and a break in slope as predicted by the theory. The multitude of data points well above the lines is the result of energetic events having other mechanisms for their source; the wind-forced motions thus set a lower bound on the tilt variance. It should be reiterated that the theory for the wind-induced motions predicts that these are not waves but deformations that move downwind at the wind speed, as discussed by *DiMarco et al.* [1991]. Note that in Figure 6 the horizontal velocities are significantly less than the vertical ones. With only one sensor station on the refrozen lead, it was not possible to tell whether these were locally forced motions moving in the direction of and at the wind speed or were waves traveling on the flexural-gravity wave dispersion surface.

Flexural Waves

The motions in the band around 1 Hz are dominated by episodes of waves generated during periods of ridge building on the boundaries of the floe. A representative time series from a geophone during one of these events is shown in Figure 9, along with the corresponding spectrum. The direction of propagation of these waves often can be discerned by the relative amplitudes of the orthogonal horizontal channels at a single station (as was done for the gravity waves) and/or the limited array formed by the two geophone stations. The proof that these are flexural waves is provided by Figure 4, which is the dispersion relation calculated from the phase function of the cross spectrum between the vertical channels of two geophone stations. The theoretical curve that best fits the data has a value for the flexural rigidity of 3 GN m, which is less than but reasonably consistent with the value calculated from the ice core data. (The accuracy of the accompanying value of Young's modulus is the subject of a separate communication [*DiMarco et al.*, 1992].) The direction of this particular group of waves was along the axis between

the two stations, but at other times waves were observed from all directions in the vicinity of the active side of the floe. The expected phase relation between the vertical axis and the aligned horizontal axis on either of the geophone stations is retrograde with 90° phase shift, as expected for a flexural wave.

Thus the largest vertical ice velocities in the band of 1–10 Hz are represented by flexural waves. These waves come in groups which are highly intermittent, both on the small scale as exhibited in the time series in Figure 9, and on the longer time scale of the data collection period. This latter conclusion is that of watch standers and cannot be determined quantitatively from the data in hand; a time series of the variance in this band cannot be plotted for the duration of the experiment because data collection at the high rate was intermittent. There was a qualitative correlation with the ridging events, and no observed correlation with the local wind speed.

Acoustic and/or Elastic Waves

There is an evident change in the spectral form in Figure 1 near 20 Hz. There is a break in the slope of the spectrum and a significant decrease in the variance of spectral level, i.e., in the range bounded by the upper and lower percentile curves. These are indicative of a change in the dominant process causing the motions at the lower frequencies vis à vis the process at the higher frequencies.

A scrutiny of the data set shows that there are times when the energy level in the band above 10 Hz is correlated with

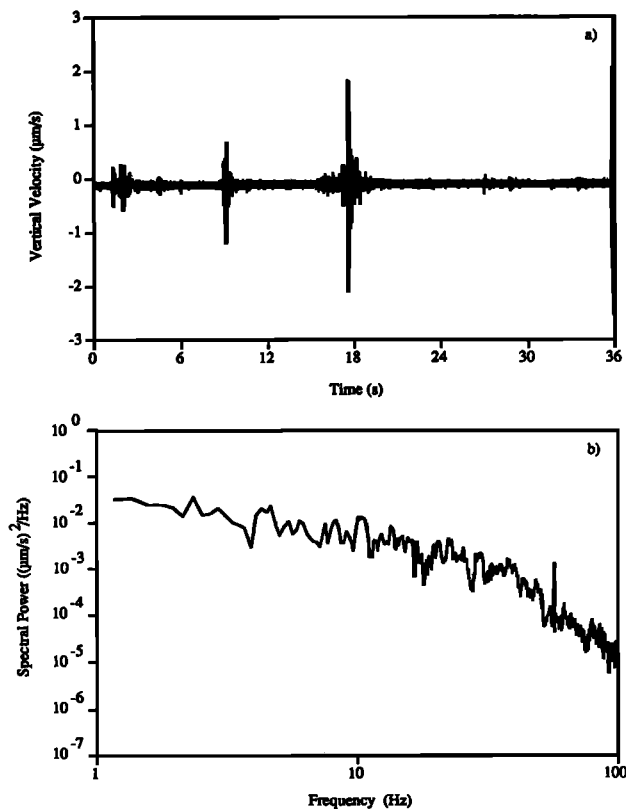


Fig. 9. Sample of vertical geophone data (vertical velocity) during ridge-building event on boundary of ice floe. (a) Time series. (b) Spectrum.

the energy level below 10 Hz (i.e., Figure 9). Thus the level of the higher-frequency motions often rises in proportion to the lower-frequency motion when there is a ridging event on the floe. On the other hand, there are times when this band is raised while the lower-frequency one is not. Figure 10 is a sample time series and spectrum of a geophone for this latter case. The time series is much less intermittent than in the case of high-energy events shown in Figure 9 (note the change in vertical scale), and there is a weak spectral break in slope near 10 Hz, leading us to conclude that there is a change in the dominant mechanism near that frequency. The specific evidence for a change in the mode of propagation is rather weak and is discussed below. In brief, we conclude the energy at high frequencies in this case has arrived through propagation in the water, having been generated from ridging events on floes remote from our instrumented floe.

The first piece of evidence is that the energy level at high frequencies is not as intermittent as that in the lower-frequency band. The data do not exhibit the very large changes in level which occur when ridging is on the same floe as the instruments. If the smaller signals emanate from remote locations, the effective source will be spread over a larger area and there will be more of these events occurring. Thus the law of large numbers applies, and the data will exhibit a more nearly Gaussian distribution. Note the change in stationarity between Figures 9a and 10a.

The second piece of evidence supporting the hypothesis is the cross spectrum between geophone stations. The phase function is completely random, and no specific wave speed

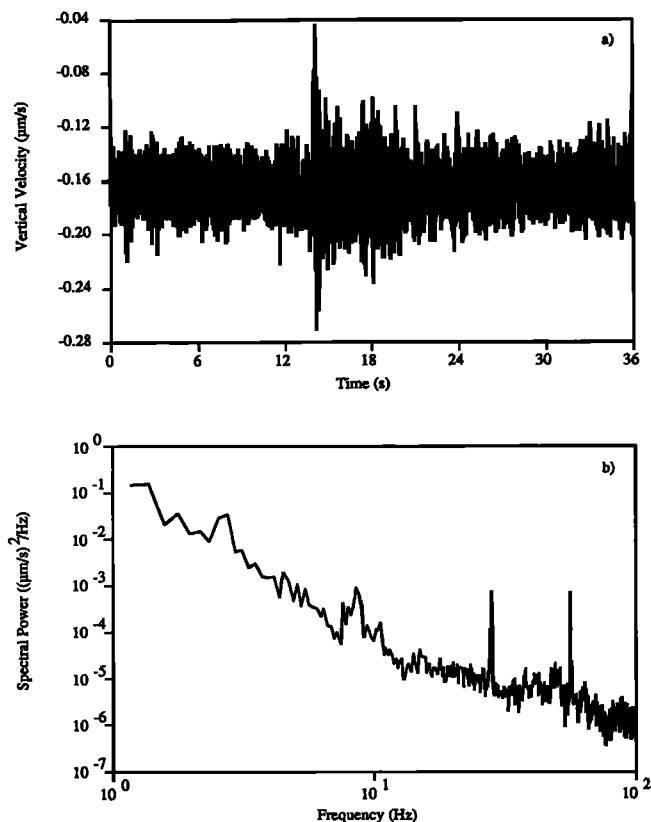


Fig. 10. Sample of vertical geophone data for noise from more distant sources. (a) Time series. (b) Spectrum.

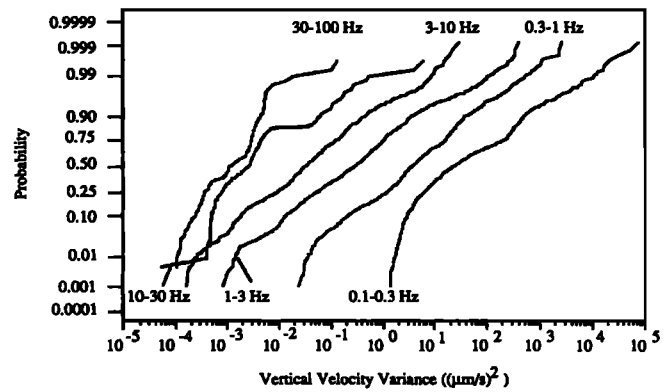


Fig. 11. Cumulative distribution functions for six frequency bands. The ordinate is plotted so that a straight line indicates Gaussian distribution of data points (see text).

can be discerned. This result could occur for one of several reasons. Either the waves are much more omnidirectional, or there is a mixture of modes of propagation. We have no direct evidence to choose between these reasons, but again we hypothesize that the former answer is the correct one. If the vibrations are generated on other floes, one does expect that the dominant mode would be through the water, with the surface moving only as the upper boundary from which a good percentage of the energy is reflected. Because of their larger numbers, the direction of arrival would be random.

The variance in the 10- to 100-Hz band did not display any noticeable correlation with the local wind speed, as did the band near 0.2 Hz on thin ice. However, a band near 1 kHz and above (not included in Figure 1) exhibited a "hiss" on the geophones during wind speeds above about 7 m/s, presumably due to ice crystals being moved by the wind [Milne et al., 1967]. The band above 100 Hz also exhibited an increase in level during one period of significant surface cooling during the observation period due to thermal cracking, as was observed previously on hydrophones by Milne [1972] and others.

The distribution function of energy is of interest because of the intermittence of local generation events. Figure 11 is a plot of the cumulative distribution function of variance of vertical velocity in six frequency bands from 0.1 to 100 Hz. The large changes in level dictate that we use the logarithm of energy on the ordinate. A straight line on this plot represents a Gaussian distribution on a linear scale of the ordinate. Thus the observed variance is consistent with a lognormally distributed variate. Also, the slope of the line is a direct measure of the variance of the energy level, or the degree of intermittence. Taking the bands in turn, the rightmost line in the band 0.1–0.3 Hz has the most energy and the most variance in level. On the other hand, about 25% of the data are contaminated by noise. (This is indicated by the nearly vertical line which bounds the lower energy levels. This high percentage of time in noise is caused by the much reduced amplitude response of the geophone at low frequencies. This also indicates that the 10% line in this band in Figure 1 is contaminated by sensor noise.) The data above the noise are well represented by a lognormal distribution. The higher-frequency bands have lower median energy and lower variance. Above 10 Hz the variance is reduced so that we cannot distinguish between a lognormal or a Gaussian

variate. The raggedness of the high-frequency curves results from the rather limited number of samples (see Table 1). Although the levels are representative, the details of the curve are not indicative of general trends because of small sample statistics.

CONCLUSIONS

Observations of the vibrations of Arctic pack ice as quantified by the vertical velocity measured by geophones and accelerometers display a rich variety of natural physical processes. Gravity waves from the open ocean propagate across the floe, motions are forced locally by atmospheric pressure fluctuations associated with turbulence in the wind, flexural waves generated by local ice ridging events propagate across the floe, and elastic motions are induced by waterborne sound arriving from more distant ridging events. The gravity and flexural waves have been well characterized by measurements of their dispersion relation. The wind motions are in reasonable agreement with a recent model for the response of an ice sheet to atmospheric turbulence. Finally, the acoustic motions are consistent with a hypothesis of noise sources remote from the experiment floe. Reasonable bounds have been identified for the respective frequency bands in which each mechanism is dominant, and spectral shapes and distribution functions of the energy level in specific bands have been determined across the frequency range 0.01–100 Hz.

Acknowledgments. This research was supported in part by the Arctic Sciences Program of ONR under contract N00014-90-C-0163, and the Scientific Officer, Tom Curtin, is gratefully acknowledged for his encouragement and support.

REFERENCES

- Buck, B. M., and J. H. Wilson, Nearfield noise measurements from an Arctic pressure ridge, *J. Acoust. Soc. Am.*, **80**, 256–264, 1986.
- Crary, A. P., A brief study of ice tremors, *Bull. Seismol. Soc. Am.*, **45**, 1–9, 1955.
- Crary, A. P., Arctic ice island research, *Adv. Geophys.*, **3**, 1–41, 1956.
- Crary, A. P., R. D. Cotell, and J. Oliver, Geophysical studies in the Beaufort Sea, 1951, *Eos Trans. AGU*, **33**, 211–216, 1952.
- Crocker, G. B., and P. Wadhams, Observations of wind-generated waves in Antarctic fast ice, *J. Geophys. Res.*, **93**, 1292–1299, 1988.
- DiMarco, R. L., J. P. Dugan, and W. W. Martin, Ice motions forced by boundary layer turbulence, *J. Geophys. Res.*, **96**, 10,617–10,624, 1991.
- DiMarco, R. L., W. W. Martin, J. P. Dugan, and W. J. Tucker, Sea ice flexural rigidity: A comparison of static and dynamic methods, *Cold Reg. Sci. Technol.*, in press, 1992.
- Dyer, I., The song of sea ice and other ocean melodies, in *Arctic Technology and Policy*, edited by I. Dyer and C. Chrystostomidis, pp. 11–37, Hemisphere, New York, 1983.
- Ewing, M., and A. P. Crary, Propagation of elastic waves in ice, II, *Physics*, **5**, 181–184, 1934.
- Ganton, J. H., and A. R. Milne, Temperature- and wind-dependent ambient noise under midwinter pack ice, *J. Acoust. Soc. Am.*, **38**, 406–411, 1965.
- Greene, C. R., and B. M. Buck, Arctic Ocean ambient noise, *J. Acoust. Soc. Am.*, **36**, 1218–1220, 1964.
- Hunkins, K., Seismic studies of sea ice, *J. Geophys. Res.*, **65**, 3459–3472, 1960.
- Hunkins, K., Waves in the Arctic Ocean, *J. Geophys. Res.*, **67**, 2477–2489, 1962.
- LeSchack, L. A., and R. A. Haubrich, Observations of waves on an ice-covered ocean, *J. Geophys. Res.*, **69**, 3815–3821, 1964.
- Makris, N. C., and I. Dyer, Environmental correlates of pack ice noise, *J. Acoust. Soc. Am.*, **79**, 1434–1440, 1986.
- Milne, A. R., Thermal tension cracking in sea ice: A source of underice noise, *J. Geophys. Res.*, **77**, 2177–2192, 1972.
- Milne, A. R., J. H. Ganton, and D. J. McMillin, Ambient noise under sea ice and further measurements of wind and temperature dependence, *J. Acoust. Soc. Am.*, **41**, 525–528, 1967.
- Munk, W. H., F. E. Snodgrass, and M. J. Tucker, Spectra of low-frequency ocean waves, *Bull. Scripps Inst. Oceanogr.*, **7**(4), 283–362, 1959.
- Oliver, J., A. P. Crary, and R. Cotell, Elastic waves in Arctic pack ice, *Eos Trans. AGU*, **35**, 282–292, 1954.
- Pritchard, R. S., Arctic Ocean background noise caused by ridging of sea ice, *J. Acoust. Soc. Am.*, **75**, 419–427, 1984.
- Robin, G. de Q., Wave propagation through fields of pack ice, *Philos. Trans. R. Soc. London Ser. A*, **255**, 313–339, 1963.
- Smirnov, V. N., and E. M. Lin'kov, On a source of high frequency seismic disturbances and flexural-gravitational waves in the Antarctic, *Izv. Acad. Sci. USSR. Phys. Solid Earth*, Engl. Transl., **8**, 542–545, 1967.
- Squire, V. A., Wind over ice: A mechanism for the generation of ice coupled waves, in *Ice Technology, Proceedings, 1st International Conference*, edited by T. Murthy, J. Connor, and C. Brebbia, pp. 115–128, Springer-Verlag, New York, 1986.
- Wadhams, P., Attenuation of swell by sea ice, *J. Geophys. Res.*, **78**, 3552–3563, 1973.
- Wadhams, P., V. A. Squire, D. J. Goodman, A. M. Cowan, and S. C. Moore, The attenuation rates of ocean waves in the marginal ice zone, *J. Geophys. Res.*, **93**, 6799–6818, 1988.

R. L. DiMarco and W. W. Martin, Areté Associates, P.O. Box 16287, Arlington, VA 22215.
J. P. Dugan, ONR European Office, PSC 802, Box 39, FPO AI 04999.

(Received March 21, 1991;
revised January 6, 1992;
accepted January 13, 1992.)